

Lifelong Learning for Neural powered Mixed Integer Programming

Sahil Manchanda, Sayan Ranu

Department of Computer Science and Engineering
Indian Institute of Technology, Delhi
{sahil.manchanda,sayanranu}@cse.iitd.ac.in

Abstract

Mixed Integer programs (MIPs) are typically solved by the Branch-and-Bound algorithm. Recently, *Learning to imitate* fast approximations of the expert *strong branching* heuristic has gained attention due to its success in reducing the running time for solving MIPs. However, existing learning-to-branch methods assume that the entire training data is available in a single session of training. This assumption is often not true, and if the training data is supplied in continual fashion over time, existing techniques suffer from *catastrophic forgetting*.

In this work, we study the hitherto unexplored paradigm of *Lifelong Learning to Branch* on Mixed Integer Programs. To mitigate catastrophic forgetting, we propose LiMIP, which is powered by the idea of modeling an MIP instance in the form of a bipartite graph, which we map to an embedding space using a bipartite Graph Attention Network. This rich embedding space avoids catastrophic forgetting through the application of knowledge distillation and elastic weight consolidation, wherein we learn the parameters key towards retaining efficacy and are therefore protected from significant drift. We evaluate LiMIP on a series of NP-hard problems and establish that in comparison to existing baselines, LiMIP is up to 50% better when confronted with lifelong learning.

1 Introduction and Related Work

Combinatorial optimization (CO) is a subclass of optimization problems that deals with optimizing a certain objective function by selecting a subset of elements from a finite set. Although CO problems are generally NP-hard (Taha 2014) from a complexity theory viewpoint, still they are solved routinely in diverse fields such as capacity planning, resource allocation, scheduling, and manufacturing (Taha 2014). It is common to formulate most of these CO problems as Mixed integer programs (MIPs) (Achterberg 2007). However, these MIPs are difficult to solve due to the non-convexity of their feasible region. Instead of solving it directly, their LP-relaxed versions are solved (Achterberg 2007). Modern solvers such as SCIP (Gamrath et al. 2020) employ the Branch-and-Bound (B&B) (Achterberg 2007) algorithm to solve these MIPs. B&B recursively partitions the solution space into a search tree and then prunes subtrees that provably cannot generate an optimal solution. This is an iterative process, which consists of making sequential

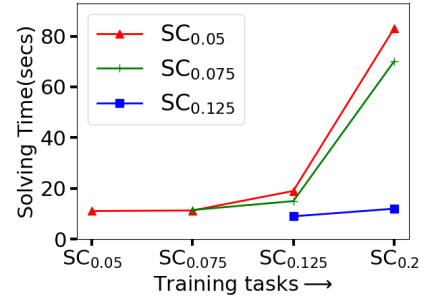


Figure 1: Illustration of catastrophic forgetting on SoA method (Gasse et al. 2019) on Set Cover dataset. The plot shows the rapid increase in the geometric mean of solving time on instances of past problems when the model is further trained *sequentially* on instances of a new problems.

decisions such as node selection, branching variable selection, etc., to direct the search procedure. The efficiency of the B&B algorithm mainly depends upon the branching variable selection and node selection (Achterberg 2007). In this work, we focus on the former. In modern MIP solvers (Gamrath et al. 2020), the branching variable decisions are generally based upon hard-coded heuristics designed by experts to direct the search process to solve an MIP (Achterberg 2007). Among various heuristics, *strong branching* is one such heuristic that is highly effective in reducing the size of Branch-and-Bound tree (Achterberg 2007; Gasse et al. 2019). However, its main disadvantage is the extremely high computational cost associated with choosing the best variable to branch. Hence, it is rarely used in practice (Achterberg 2007; Huang et al. 2021).

In order to utilize the advantage of the powerful strong branching heuristic, however at a lower computational cost, recently, multiple algorithms have been developed (Gasse et al. 2019; Khalil et al. 2016; Nair et al. 2020; Gupta et al. 2020). At their core, they use *imitation learning* to learn *fast approximations* of the *strong branching* heuristic on a family of MIP instances. These algorithms estimate scores of branching candidate variables quickly on unseen but similar MIP instances. This paradigm is popularly known as *learning to branch*. These methods have obtained signifi-

cant gains in terms of problem solving time over modern MIP solvers such as SCIP.

Despite significant success, existing techniques on learning to branch are limited by the assumption that the entire training data is available in single session of training.

This assumption is not realistic in the context of MIPs as the semantics of CO problems may keep changing with time. Consequently, the data to train the *learning-to-branch* model is dynamic with updates arriving sequentially over time. The above scenario is commonly observed in industries such as shipping and food delivery where entities, such as service locations and warehouses, get added/removed over time. Further, the semantics of the problem such as the demand, supply, customer distribution, facility constraints etc. also fluctuate. Hence, to tackle such scenarios, the model should be capable of learning in an incremental fashion as more data appears over time as retraining the entire model again can be computationally expensive.

The ability to continually learn over time is referred to as *lifelong/continual learning* (Parisi et al. 2019). This aligns with the ability of humans to continually acquire skills throughout their lifespan. Lifelong learning aspires to gain more knowledge sequentially and improve existing model as more data arrives. However, the quintessential failure model of lifelong learning on neural models is *catastrophic forgetting* i.e when new concepts are learned sequentially, the neural model forgets the concepts it learned previously (Kirkpatrick et al. 2017; Parisi et al. 2019)¹.

In this context, we analyze the performance of the state-of-the-art learning-to-branch technique GCNN (Gasse et al. 2019) in the lifelong learning scenario, i.e., training the model sequentially on different problems. In Fig. 1 we observe that the solving time on instances of the SetCover (SC) problem with edge-probability 0.05, i.e., $SC_{0.05}$ increases significantly when the parameters of the model are updated sequentially using training data of $SC_{0.075}$, $SC_{0.125}$ and $SC_{0.2}$ ². Similar phenomenon is observed on other problems in the sequence such as $SC_{0.075}$, etc. It can be clearly concluded from Fig. 1 that GCNN (Gasse et al. 2019) suffers from catastrophic forgetting in the lifelong learning scenario.

In the context of MIPs, a lifelong learning paradigm, due to its nature, promotes efficient learning since retraining from scratch is costly (Parisi et al. 2019), especially on industrial level MIPs where the number of variables and constraints are in orders of millions (Nair et al. 2020). Further, such a paradigm of *continually gaining competencies* on different problems, offers opportunity to transfer the gained knowledge to unseen as well as previously seen problems. Owing to knowledge sharing across problems, these models cope better with low availability of training data. Learning from low-volume training data is important in the context of MIPs since generating training data (state-action pairs) itself is a computationally expensive process (Nair et al. 2020). Finally, using a single model that is updated regularly with various competencies, instead of maintaining multiple

problem-specific models is desired as it is memory efficient with lower maintenance overhead.

Motivated by the above listed benefits of lifelong learning, in this work we focus on the novel paradigm of *Lifelong Learning to Branch in Mixed Integer Programs*. Our core contributions are as follows.

- **Problem Formulation:** We present the paradigm of Lifelong Learning to Branch in Mixed Integer Programs. To the best of our knowledge, we are the first to investigate this paradigm.
- **Investigation of catastrophic forgetting:** We conduct an empirical investigation of the SoA method (Gasse et al. 2019) and demonstrate that it suffers from catastrophic forgetting when it learns to branch on different problems in succession.
- **Novel Algorithm:** We propose LIMIP, a Lifelong Learning method to solve Mixed Integer Programs. LIMIP encodes the state-space of a problem through an *edge-weighted, bipartite Graph Attention Network*. To mitigate catastrophic forgetting, LIMIP utilizes a novel combination of *Knowledge Distillation* and *Elastic Weight Consolidation* to shield the key parameters of previously learned problems from significant drift.
- **Experimental Evaluation:** We conduct empirical evaluation on a series of NP-hard problems with *drifting* data distribution and evolving constraints. We establish that LIMIP is effective in learning to solve MIPs in a lifelong fashion and overcomes the problem of catastrophic forgetting. Further, it is also capable of transferring the gained knowledge effectively to NP-hard problems with very limited amount of training data.

2 Preliminaries

Definition 1 (Mixed Integer Program). *A mixed-integer linear program is an optimization problem of the form:*

$$\begin{aligned} & \text{minimize } \mathbf{c}^\top \mathbf{x} \\ & \text{subject to } \mathbf{A}\mathbf{x} \leq \mathbf{b} \\ & \mathbf{l} \leq \mathbf{x} \leq \mathbf{u} \\ & \mathbf{x} \in \mathbb{Z}^p \times \mathbb{R}^{n-p}, \end{aligned}$$

where n is the total number of variables, p is the number of integral variables. $\mathbf{x} \in \mathbb{Z}^p \times \mathbb{R}^{n-p}$, $\mathbf{A} \in \mathbb{R}^{m \times n}$ is the constraint coefficient matrix, $\mathbf{b} \in \mathbb{R}^m$, right hand side constraint coefficient vector, $\mathbf{c} \in \mathbb{R}^n$ is the objective coefficient vector. Further, the variables $\mathbf{l}, \mathbf{u} \in \mathbb{R}^n$ represent the lower and upper variable bound vectors.

MIPs are solved widely using Branch-and-Bound (B&B) technique, which relaxes the integrality constraints and obtains a continuous linear program (LP). The LP is solved efficiently using the simplex algorithm (Achterberg 2007). In case the relaxed solution is also integral and respects all the constraints, then it is also a solution to the problem (not necessarily optimal). Otherwise B&B decomposes the LP relaxation into two sub-problems, by splitting the feasible region based upon a variable that does not respect integrality constraints in the current LP solution x^* . Specifically,

$$x_i \leq \lfloor x_i^* \rfloor \vee x_i \geq \lceil x_i^* \rceil, \quad \exists i \leq p \mid x_i^* \notin \mathbb{Z},$$

¹Detailed related work present in Appendix A.1

²Details of the dataset in Experimental Section

The B&B solving process repeatedly performs decomposition generating a search tree. The process stops if both the upper and lower bounds are equal or when the feasible regions do not decompose anymore, which is a certificate of infeasibility or optimality. This B&B procedure involves an extremely important step of selecting the fractional *decision* variable to branch upon from the set of candidate variables \mathcal{C} . The chosen variable is used to partition the search space and has a significant impact on the size of the resulting search tree (Achterberg 2007).

Among several heuristics available to choose the branching variable, *strong branching* is widely known to produce the smallest B&B trees. It calculates the expected bound improvement for each candidate variable before performing branching. Although it produces the smallest B&B trees, strong branching requires computing the solution of two LPs for each candidate variable. The cost of finding the best variable is prohibitively high and hence strong branching is not used in practice.

In the B&B setup, the MILP solver is considered to be the *environment*, and the brancher the *agent* (Khalil et al. 2016; Gasse et al. 2019). At the t^{th} decision step, the solver is in state s_t , which comprises the B&B tree with all past branching decisions (Gasse et al. 2019), the best integer solution found so far, the LP solution of each node, the currently focused leaf node, as well as any other solver statistics (for example, the number of times every primal heuristic has been called). In the context of strong branching, at a given state s_t , let a_t be the variable chosen by strong branching among the set of all candidate variables \mathcal{C} . Based upon the above discussion, we now define the problem of *Learning to Branch*.

Problem 1 (Learning to Branch). *For a B&B tree, at the t^{th} decision step of the solver, let the solver be in state s_t and a decision to choose a variable to branch is to be made from a set of candidate variables. Given a collection of state-action (s_t, a_t) pairs obtained from running strong branching, the goal is to learn a scoring function f parameterized by θ that imitates branching decisions made by the strong branching expert.*

Since in our setup we aim to learn on multiple problems, therefore in this context, we refer to each problem as a task.

Problem 2 (Lifelong Learning to Branch). *Given a sequence of tasks $\mathcal{T} = [\mathcal{T}_1, \dots, \mathcal{T}_T]$ of length T , we aim to update the parameters of the model sequentially over time such that at the i^{th} task, when parameter θ_{i-1} is updated to θ_i by training using the instances of the task \mathcal{T}_i , the model avoids catastrophic forgetting on tasks \mathcal{T}_j for $j < i$. Specifically, the increase in running time on problems $\mathcal{T}_j \forall j < i$ using the updated model θ_i should be reasonably low. Additionally, the performance on newly learned tasks should also not be hindered significantly.*

3 LiMIP: Our proposed methodology

In this section we describe our proposed method LiMIP. Fig. 2 presents the overview of LiMIP. We first convert a given MIP instance to a bipartite graph. Next, we describe a method to encode the variables and constraints of MIP using an *edge-weighted, bipartite graph attention network*

(GAT). Finally, we describe the procedure of learning the parameters of the model in a lifelong fashion by avoiding catastrophic forgetting. With the outline being set, we next discuss each of these components in detail.

3.1 MIP Representation: State Encoding

Inspired from Gasse et al. (2019), to encode the state s_t of the B&B tree at timestep t , we use a bipartite graph representation $G = (\mathbf{V}, \mathbf{E}, \mathbf{C})$. One side of the graph containing n nodes represent the n variables and the other side consisting of m nodes represent the m constraints. There exists an edge between j^{th} variable node and i^{th} constraint node if j^{th} variable appears in the i^{th} constraint. The weight of an edge $e_{i,j}$ corresponds to the value of the coefficient of the variable v_j in the constraint c_i . We use $\mathbf{V} \in R^{n \times d_1}$ to represent variable features, $\mathbf{E} \in R^{n \times m \times 1}$ for edge features, and $\mathbf{C} \in R^{m \times d_2}$ to represent the constraint features. For each of the node in the graph we use the raw solver specific input features of Gasse et al. (2019), which can be found in the appendix A.4. Fig. 2 shows an example of encoding an MIP to a bipartite graph.

3.2 Policy Parameterization: Edge Weighted Bipartite GAT

Observing the weighted and bipartite nature of the graph, it is natural to parameterize the branching variable policy $f_\theta(a|s_t)$ using an *edge-weighted* bipartite GAT. Specifically, for each node in the graph, the attention layer learns to weigh each of the node’s neighbors differently based upon its importance (Vaswani et al. 2017). Since, our graph is bipartite, we perform two levels of message passing through the GAT. Specifically, first we pass message from the variable side to the constraint side to obtain rich representation of the constraint nodes as follows:

$$\mathbf{c}_i = \alpha_{i,i} \theta^C \mathbf{c}_i + \sum_{j \in \mathcal{N}(i)} \alpha_{i,j} \theta^C \mathbf{v}_j \quad (1)$$

Here, \mathbf{c}_i and \mathbf{v}_j refer to the embeddings of i^{th} constraint and j^{th} variable respectively. $\mathcal{N}(i)$ refers to the neighbors of i^{th} node. θ^C refers to MLP associated to constrained side aggregation. α represents the attention coefficient (defined later). Next, we perform message passing from constraint side to variable side. This allows us to generate richer representations for each of the variables nodes.

$$\mathbf{v}_j = \alpha_{j,j} \theta^V \mathbf{v}_j + \sum_{i \in \mathcal{N}(j)} \alpha_{j,i} \theta^V \mathbf{c}_i \quad (2)$$

θ^V refers to weights associated to the variable side aggregation. The attention coefficient α is computed as below:

$$\alpha_{i,j} = \frac{\exp\left(\rho\left(\left(\mathbf{a}^C\right)^T\left[\theta^C \mathbf{c}_i\|\theta^C \mathbf{v}_j\|\theta_e^C \mathbf{e}_{i,j}\right]\right)\right)}{\sum_{k \in \mathcal{N}(i)} \exp\left(\rho\left(\left(\mathbf{a}^C\right)^T\left[\theta^C \mathbf{c}_i\|\theta^C \mathbf{v}_k\|\theta_e^C \mathbf{e}_{i,k}\right]\right)\right)}$$

The above attention mechanism is parameterized by the weight vector \mathbf{a}^C . θ_e^C on the constraint side aggregation refers to an MLP associated with the edge features. ρ refers to the activation function³. $\alpha_{j,i}$ is defined analogously to $\alpha_{i,j}$

³We use LeakyReLU with negative slope = 0.2

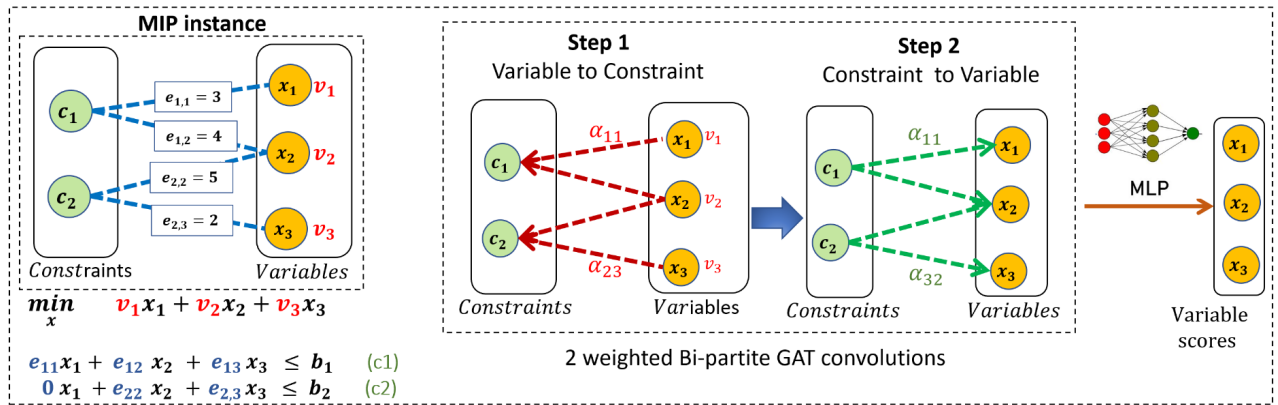


Figure 2: Bipartite graph representation of an MIP with $n = 3$ variables and $m = 2$ constraints. The bipartite graph is encoded via 2 half-aggregations of Bipartite GAT .

where C is swapped with V and the i^{th} and j^{th} nodes are interchanged.

After the two half-aggregations of eq. 1 and 2, we obtain the final representation of the candidate variable nodes. The final representation of each candidate variable node is passed through a softmax layer to obtain a probability distribution over the variables represented by $f_{\theta}(a | s_t)$. Further, to stabilize the training procedure of the bipartite-GAT, we use attention mechanism with multiple heads, details of which are present in Appendix Sec. A.5. The detailed architecture is present in Fig. 2.

3.3 Imitation Loss

Since strong branching is a powerful heuristic in reducing the size of the tree, we train the parameters θ by imitation learning of the strong branching rule.

We first collect a set of strong branching state-action pairs $\mathcal{D} = \{(s_k, a_k^*)\}_{k=1}^N$, where N is the number of branching samples collected. Then through imitation learning, we optimize the parameters θ using the following imitation loss function:

$$\mathcal{L}(\theta) = -\frac{1}{N} \sum_{(s, a^*) \in \mathcal{D}} \log f_{\theta}(a^* | s) \quad (3)$$

The optimization of the above objective encourages the neural model to predict the variable for branching which strong-branching would have chosen.

3.4 Life-Long Learning to Branch

Until now we discussed how to learn the parameters θ of the model for a given task. In this section we discuss how to learn to branch on MIPs in a lifelong fashion. As discussed earlier in Def. 2, we have a set of T problems appearing in sequence $\mathcal{T} = [\mathcal{T}_1, \dots, \mathcal{T}_T]$, and our goal is to learn the parameters sequentially over time where the training data \mathcal{D}_i for each task \mathcal{T}_i also appears sequentially. A naive solution is to update the parameters of the model sequentially as new tasks arrive. However, as we already observed in Fig. 1, if the neural model is updated in this fashion, it suffers from catastrophic forgetting on the earlier learned tasks. Hence, our goal is to update the parameters of the model on new

tasks while preserving the knowledge gained on previous tasks to avoid catastrophic forgetting.

One way to consolidate past knowledge is to replay the training data of the past tasks. However, as the number of tasks increase, it becomes computationally expensive. Further, another option of storing only a small set of labeled samples and replaying them is prone to over-fitting (Wang et al. 2020). Hence, inspired by recent works on continual learning (Buzzega et al. 2020; Wang et al. 2020), to tackle the problem of catastrophic forgetting in *lifelong learning to branch* we take the following two perspectives. First idea is to approximate the knowledge gained by the model in the past via *distillation* of model’s past behavior when learning new tasks. Second, we optimize the parameters of the model in a constrained way in order to prevent significant drift on the parameters important for previously learned tasks. Fig. 3. visually describes the process. Now, we discuss both the perspectives below in detail.

Mimicking model’s past behavior through Knowledge

Distillation: In order to maintain past learned patterns during lifelong learning, our goal is to search for model parameters that fit well on the current task and also approximate the optimal behavior of the model on the older tasks. Towards this we aim to encourage the model to mimic its original(past) output *logits* for a small number of samples of the past tasks. To accomplish this we apply *Knowledge distillation*(KD) (Buzzega et al. 2020) approach to enforce the neural network to generate similar logits that the model produced for these samples in the past during optimizing of the task to which the related sample belonged to. Mathematically,

$$\mathcal{L}_{KL} = \mathbb{E}_{(s, z) \sim M} [D_{KL}(z || f_{\theta}(s))] \quad (4)$$

Here $z = f_{\theta_j^*}(s)$ refers to the logits z of sample s and θ_j^* refers to the set of optimal parameters of task \mathcal{T}_j . These (s, z) pairs are stored in a fixed-size buffer M . Specifically, for $s \in M$, $f_{\theta_j^*}(s)$ is preserved where s is a training sample from task \mathcal{T}_j . When the lifelong learning model is at step i of the sequence \mathcal{T} , M consists of samples of past experiences(logits) for tasks seen till step $i - 1$. Further, since we

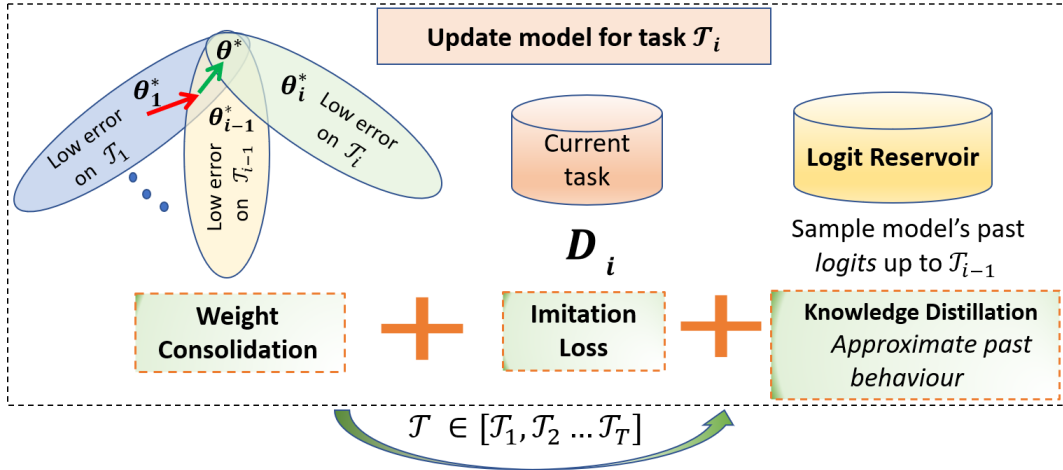


Figure 3: Architecture diagram representing the update mechanism of LiMIP at the i^{th} step of sequence \mathcal{T} .

do not have any prior information of how many tasks we will observe, we use *reservoir sampling* to preserve samples for Knowledge-Distillation. Reservoir sampling ensures that samples from all tasks are stored with equal probability in the buffer without knowing the number of tasks/samples in the stream in advance (Buzzega et al. 2020).

Preservation of model’s important parameters: As we store only a small set of logits in our memory buffer instead of the entire training data of past tasks, it is prone to over-fitting. Although, over-fitting can be tackled to an extent by L2 regularizers, the restriction imposed by L2 regularizers by constraining the entire network through a fixed coefficient is too severe and might prevent learning of the new tasks itself. Inspired from recent works (Kirkpatrick et al. 2017; Wang et al. 2020), to counter this problem, we aim to learn to adjust the magnitude of the parameter updates on certain model weights based on how important they are to the previously learned tasks. To accomplish this we apply *Elastic Weight Consolidation (EWC)* (Wang et al. 2020; Kirkpatrick et al. 2017). Specifically, after the training on a task \mathcal{T}_j is complete, we compute the importance of each parameter w on the task \mathcal{T}_j as follows:

$$\Omega_j^w = \mathbb{E}_{(s, a^*) \sim D_j} \left[\left(\frac{\delta \mathcal{L}(s, a^*)}{\delta \theta_j^w} \right)^2 \right]$$

$\mathcal{L}(s, a^*)$ refers to the loss on sample s with ground-truth a^* . The term $\frac{\delta \mathcal{L}(s, a^*)}{\delta \theta_j^w}$ calculates the gradient of the loss with respect to the parameter w learned on task \mathcal{T}_j . Ω_j^w captures the importance of weight w to task \mathcal{T}_j . We note that D_j is no more required during future tasks once the computation of Ω for task \mathcal{T}_j is complete.

Now, when a new task \mathcal{T}_i arrives, we apply the above regularization (penalize) to prevent large amount of drift on parameters important for earlier learned tasks. Here, the weights of the regularization are obtained from Ω . We ac-

complish the regularization by the below loss function.

$$\mathcal{L}_{importance} = \sum_{j=1}^{i-1} \sum_w \Omega_j^w (\theta_i^w - \theta_{j^*}^w)^2 \quad (5)$$

The above term is a quadratic penalty term on the difference between the parameters for the new and the old tasks. Ω consists of diagonal weighing proportional to the diagonal of the Fisher information metric over the old parameters on the old tasks (Liu, Yang, and Wang 2021). θ_{j^*} refers to optimal parameters of task \mathcal{T}_j . When updating parameters of the model to learn to branch on a new task \mathcal{T}_i , the above penalization will encourage the *important model* parameters to be close to the parameters obtained for earlier learned tasks $\mathcal{T}_1, \mathcal{T}_2 \dots \mathcal{T}_{i-1}$. Fig. 2 b) summarizes this concept visually through overlapping optimal parameter spaces.

Lifelong learning optimization objective: Finally, combining the loss functions of eqs. 3, 4 and 5, we obtain the optimization objective at the i^{th} step as follows

$$\begin{aligned} \mathcal{L}_{lifelong} = & \sum_{(s, a^*) \in \mathcal{D}_i} \log f_\theta(a^* | s) \\ & + \alpha \mathbb{E}_{(s, z) \sim \mathcal{M}} [D_{KL}(z || f_\theta(s))] \\ & + \beta \sum_{j=1}^{i-1} \sum_w \Omega_j^w (\theta_i^w - \theta_{j^*}^w)^2 \end{aligned}$$

The above equation while learning new tasks, consolidates past information in order to maintain stability of parameters important for previously learned tasks. α controls the weight corresponding to mimicking past logits and β controls scale of the weight consolidation regularizer.

4 Experiments

In this section we measure the effectiveness of our proposed approach LiMIP and establish:

- **Minimal forgetting:** LIMIP is capable of lifelong learning on NP-hard problems with drifting data distributions and avoids catastrophic forgetting on previously learned problems.
- **No hindrance in learning future tasks:** Despite adding constraints to prevent significant updates to the model, LIMIP does not hinder learning on new tasks.
- **Transfer to Low data regime:** We compare the performance of LIMIP to transfer on a low-training data regime task which is similar to a task LIMIP learned in the past. LIMIP effectively transfers its previously gained and *unforgotten knowledge* to the unseen task.
- **Efficient learning through Bipartite GAT:** Attributed to rich representations learned through the attention mechanism, LIMIP reduces solving time on instances when compared to GCNN (Gasse et al. 2019).

4.1 Datasets

We use the following datasets to evaluate the performance of our method against different baselines.

Set Cover: We consider the Set Cover problem of Balas and Ho (1980). Let p be the probability of an item belonging to a set in the Set Cover (SC) problem. SC_p refers to Set Cover problem with set-item probability p . To simulate lifelong learning setup, we generate multiple Set Cover problems datasets each with a different probability, i.e., $\mathcal{T} = [SC_{0.05}, SC_{0.075}, SC_{0.1}, SC_{0.125}, SC_{0.15}, SC_{0.2}]$. In all instances we set number of rows to 700 and number of columns to 800.

Independent Set : We consider the Maximum Independent Set (MIS) problem on the Barabási-Alberta graph (Albert and Barabási 2002) generated with different sizes and affinities. $IS_{A,S}$ denotes as instance where A is the affinity and S is the size of the graph. To simulate lifelong learning setup, we generate independent set problem datasets with different sizes and affinities as $\mathcal{T} = [IS_{4,750}, IS_{4,500}, IS_{4,450}, IS_{5,450}, IS_{5,400}, IS_{5,350}]$.

Facility Location with constraints: We consider the Facility Location problem (Gasse et al. 2019) and to simulate lifelong learning scenario, we use facility capacities and customer demands sampled from drifting distributions over time. This is a realistic scenario where customer demands and facility capacities keep changing over time. We define a certain task of facility location problem as $FC_{(Clow,Chigh),(Dlow,Dhigh)}$. $Clow, Chigh$ refers to the lower and upper limit of the facility capacity. $Dlow, Dhigh$ refers to the lower and upper limit of customer demand. Generating a facility location problem requires, for each facility, sampling a capacity uniformly at random from $[Clow, Chigh]$ and for each customer a demand sampled from $[Dlow, Dhigh]$. In addition to evolving customer demand and facility supply distribution, we also simulate the setting of adding new constraints. We add the constraint of the maximum number of customers that can be served by a facility and denote it by MS . We consider the following sequence of facility location problem datasets $\mathcal{T} = [FC_{(40,50),(5,10)}, FC_{(50,55),(30,35)}, FC_{(80,90),(60,65)}, FC_{(100,110),(80,90)}, FC_{(100,110),(80,90),MS=95}]$. In all cases, we set the number of customers and facilities to 100. The

detailed procedure to generate these instances is described in Appendix A.6.

These datasets are challenging for state-of-the-art solvers, and also representative of the types of integer programming problems encountered in practice.

4.2 Experimental Setup and Parameters

We use SCIP (Gamrath et al. 2020) as the backend solver, with a time limit of 45 minutes. We use a system running on Intel Xeon 6248 processor with 96 cores and 1 NVIDIA A100 GPU with 40GB memory for our experiments. Similar to existing works (Gasse et al. 2019), we enable cutting planes at the root node and deactivate solver restarts. We keep all other SCIP parameters to default. We use attention mechanism with 2 heads. We set the default buffer size to 500. We set α and β in eq. 6 to 1.5 and 100 respectively. For details of all parameters and system settings, we refer to App. A.7.

Training data generation: For each task, we generate 150,000 branching samples extracted using 10,000 generated instances for training and 30000 validation/test samples generated using 2000 instances.

Metrics: We perform evaluation on 20 different test instances using 5 different SCIP seeds. We report the standard benchmark metric for MILP benchmarking, i.e., the geometric mean of the **running time** of the solver. Additionally, we report the **hardware independent node count** (in Appendix A.9). We compute the average per-instance standard deviation so a value $X \pm s\%$ means it took X secs to solve an instance and while solving one of those instances the time varied by s on an average.

Baselines: We compare our work LIMIP with the state-of-the-art method for learning to branch GCNN (Gasse et al. 2019). We skip comparison with Zarpellon et al. (2020) since it approximates the weaker reliability pseudocost branching heuristic, which has been shown to have an inferior performance in terms of running time (See Appendix A.11). Further, we skip comparison with Gupta et al. (2020) since its focus is on developing CPU based version of learning to branch, which is out of scope of our work. For the sake of completion, we compare with the default SCIP Solver and strong branching in App. A.10.

In the context of lifelong learning, we compare with (1) Fine-tuning (FT) i.e directly updating the model on new tasks as they arrive, (2) Experience Replay (ER) and (3) Elastic Weight Consolidation (EWC) (Kirkpatrick et al. 2017). Details of baseline are present in App. A.8.

4.3 Evaluation in Lifelong Learning Scenario

Evaluating forgetting: In Fig. 4 and Fig. 5, in each subplot we study the performance of different methods on test instances of each dataset in the lifelong sequence \mathcal{T} . Specifically, each subplot in these figures refer to a test task and the x-axis shows the sequence of training tasks in the lifelong setup. We observe that as training progresses on different problems in the lifelong setup, the performance of GCNN (FT) (Gasse et al. 2019) on old problem deteriorates significantly. The older the task, the worse is the deterioration. For

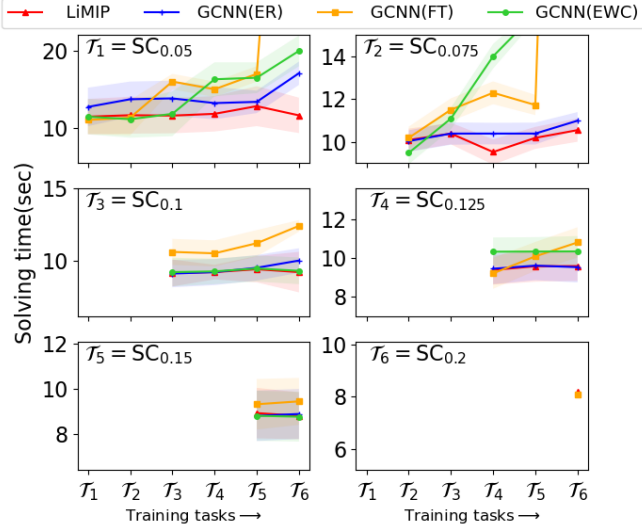


Figure 4: **Testing on Set Cover in lifelong scenario:** Evolution of solving time for each task when different methods are updated on each task sequentially. Different *evaluation tasks* are shown in *different subplots*. The x-axis denotes the sequence of training tasks and the y-axis denotes the geometric mean of solving time for *test instances* of each task in the sequence. The shaded area refers to standard deviation.

example, since $SC_{0.05}$ (top, left in Fig. 4) is trained first, it witnesses maximum increase in time across algorithms except the proposed LiMIP. This clearly shows that GCNN suffers from catastrophic forgetting when its parameters are updated on new tasks. In sharp contrast, LiMIP is able to maintain the learned patterns of past tasks when learning new tasks. This is attributed to the *knowledge distillation* loss, which helps in promoting the model to mimic past be-

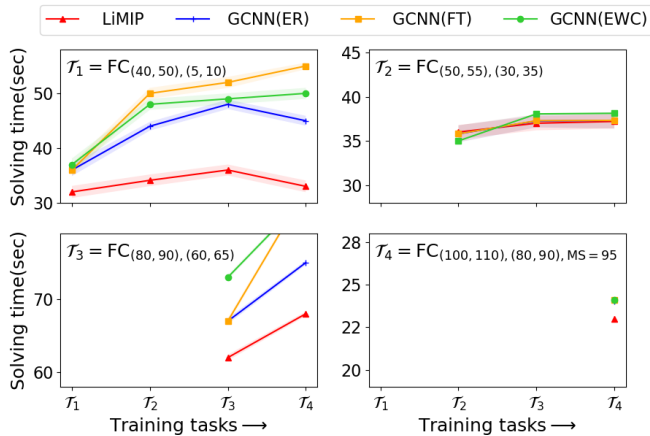


Figure 5: **Testing on Facility location in lifelong scenario:** Evolution of solving time for each task when different methods are updated on each task sequentially.

Model	Time	# Nodes
GCNN $SC_{0.047}$	16.01	607
Bipartite GAT $SC_{0.047}$	17.06	702
Bipartite GAT(FT) + $SC_{0.047}$	16.07	702
LiMIP	15.05	602
LiMIP + ($SC_{0.047}$)	14.05	441

Table 1: **Transferability performance:** Test performance comparison of fine-tuned model against model trained from scratch on the $SC_{0.047}$ dataset. LiMIP and Bipartite GAT (FT) were trained sequentially on $[SC_{0.05}, SC_{0.075}, SC_{0.1}, SC_{0.125}, SC_{0.15}, SC_{0.2}]$ and then fine-tuned on $SC_{0.047}$

havior and the *weight consolidation penalty* term which prevents significant drift on important parameters.

Low hindrance on future tasks: While avoiding catastrophic forgetting is one of the aims of lifelong learning, it should not be at the cost of learning new tasks. From Fig. 4 and Fig. 5, we observe that, while LiMIP does not forget the knowledge it gained in the past, still it does it without impacting future tasks. We can clearly see that on future tasks too LiMIP obtains superior performance compared to existing baselines.

For the sake of completeness, in App. A.12 we also compare with GAT (FT), GAT (EWC) and GAT (ER). Due to space limitation, the results on Independent Set Problem are present in App. A.10. Comparison with respect to the hardware independent node count is present in A.10.

4.4 Transferability on low data regimes

As a model learns on more tasks and gains several competencies, it can be utilized as a *weight initializer* to learn on an unseen task with low availability of training data, especially in the case of strong branching where obtaining training data is costly. To test the performance of LiMIP on transfer learning, we create a new dataset $SC_{0.047}$ with only 300 branching samples for training. This number is extremely low compared to other datasets where number of samples = 150000. We perform lifelong learning on $\mathcal{T} = [SC_{0.05}, SC_{0.075}, SC_{0.1}, SC_{0.125}, SC_{0.15}, SC_{0.2}]$ and then fine-tune on $SC_{0.047}$. We compare it with training a model from scratch on the 300 branching samples of $SC_{0.047}$. In Table 1, we study the performance gain obtained using a fine-tuned lifelong learned model vs. a model learned from scratch (GCNN $SC_{0.047}$). We observe that on an average the running time of the LiMIP method fine-tuned on $SC_{0.047}$ model is significantly better than the model trained from scratch.

4.5 Ablation studies

GCN vs Bipartite GAT: In this section we study the impact of using our Bipartite GAT compared to mean pool based GCNN. In Table 2 we observe that Bipartite GAT improves over GCNN by a small margin in terms of both running time and number of tree nodes.

Impact of regularizer on lifelong learning: In Appendix A.12, we study the impact of weight regularization on the

Dataset	Method	Time	Nodes
$SC_{0.2}$	Bipartite GAT	7.9 ± 2.56	87.2 ± 15.31
	GCNN	8.21 ± 2.45	91.2 ± 13.61
$IS_4, 750$	Bipartite GAT	22.25 ± 1.24	555.6 ± 6.02
	GCNN	25.73 ± 1.32	672.2 ± 6.2
$FC_{(40,50),(5,10)}$	Bipartite GAT	33.94 ± 1.11	246.10 ± 4.02
	GCNN	35.14 ± 1.30	248.20 ± 4.70

Table 2: Performance comparison between Bipartite GAT and GCNN encoding.

overall performance of the model.

Performance against buffer size: In Appendix A.12 we study the performance of LiMIP and ER against the size of the buffer.

5 Conclusion

Learning-to-Branch techniques have shown significant success in reducing the solving time of Mixed Integer Programs. Although, significant progress has been made, the paradigm of *learning to branch* in a *lifelong fashion* was unexplored. In this work we first examined the behavior of existing techniques in the lifelong learning scenario and discovered that they suffer from catastrophic forgetting. To tackle this problem, in this work we study the hitherto unexplored paradigm of *Lifelong Learning to Branch* on Mixed Integer Programs. We propose a method LiMIP powered by a Bipartite GAT to encode MIP instances. Further, to mitigate catastrophic forgetting, we apply *knowledge distillation* and *elastic weight consolidation* to shield key parameters from drifting and thereby retaining efficacy. Through extensive experiments on multiple NP-hard problems, we established that LiMIP is able to mitigate forgetting significantly better compared to existing baselines when confronted with lifelong learning. Additionally, the proposed method does not hinder the performance on future learning tasks too.

References

Achterberg, T. 2007. Constraint integer programming.

Albert, R.; and Barabási, A.-L. 2002. Statistical mechanics of complex networks. *Reviews of modern physics*, 74(1): 47.

Aljundi, R.; Babiloni, F.; Elhoseiny, M.; Rohrbach, M.; and Tuytelaars, T. 2018. Memory aware synapses: Learning what (not) to forget. In *Proceedings of the European Conference on Computer Vision (ECCV)*, 139–154.

Alvarez, A. M.; Louveaux, Q.; and Wehenkel, L. 2014. A supervised machine learning approach to variable branching in branch-and-bound. In *In ecml*. Citeseer.

Alvarez, A. M.; Louveaux, Q.; and Wehenkel, L. 2017. A machine learning-based approximation of strong branching. *INFORMS Journal on Computing*, 29(1): 185–195.

Balas, E.; and Ho, A. 1980. Set covering algorithms using cutting planes, heuristics, and subgradient optimization: a computational study. In *Combinatorial Optimization*, 37–60. Springer.

Banitalebi-Dehkordi, A.; and Zhang, Y. 2021. ML4CO: Is GCNN All You Need? Graph Convolutional Neural Networks Produce Strong Baselines For Combinatorial Optimization Problems, If Tuned and Trained Properly, on Appropriate Data. *arXiv preprint arXiv:2112.12251*.

Buzzega, P.; Boschini, M.; Porrello, A.; Abati, D.; and Calderara, S. 2020. Dark experience for general continual learning: a strong, simple baseline. *Advances in neural information processing systems*, 33: 15920–15930.

Chaudhry, A.; Ranzato, M.; Rohrbach, M.; and Elhoseiny, M. 2018. Efficient lifelong learning with a-gem. *arXiv preprint arXiv:1812.00420*.

Draeos, T. J.; Miner, N. E.; Lamb, C. C.; Cox, J. A.; Vineyard, C. M.; Carlson, K. D.; Severa, W. M.; James, C. D.; and Aimone, J. B. 2017. Neurogenesis deep learning: Extending deep networks to accommodate new classes. In *2017 International Joint Conference on Neural Networks (IJCNN)*, 526–533. IEEE.

Febrinanto, F. G.; Xia, F.; Moore, K.; Thapa, C.; and Aggarwal, C. 2022. Graph Lifelong Learning: A Survey. *arXiv preprint arXiv:2202.10688*.

Gamrath, G.; Anderson, D.; Bestuzheva, K.; Chen, W.-K.; Eifler, L.; Gasse, M.; Gemander, P.; Gleixner, A.; Gottwald, L.; Halbig, K.; et al. 2020. The SCIP optimization suite 7.0.

Gasse, M.; Chételat, D.; Ferroni, N.; Charlin, L.; and Lodi, A. 2019. Exact combinatorial optimization with graph convolutional neural networks. *Advances in Neural Information Processing Systems*, 32.

Gupta, P.; Gasse, M.; Khalil, E.; Mudigonda, P.; Lodi, A.; and Bengio, Y. 2020. Hybrid models for learning to branch. *Advances in neural information processing systems*, 33: 18087–18097.

Huang, L.; Chen, X.; Huo, W.; Wang, J.; Zhang, F.; Bai, B.; and Shi, L. 2021. Branch and bound in mixed integer linear programming problems: A survey of techniques and trends. *arXiv preprint arXiv:2111.06257*.

Khalil, E.; Le Bodic, P.; Song, L.; Nemhauser, G.; and Dilkina, B. 2016. Learning to branch in mixed integer programming. In *AAAI*, volume 30.

Kirkpatrick, J.; Pascanu, R.; Rabinowitz, N.; Veness, J.; Desjardins, G.; Rusu, A. A.; Milan, K.; Quan, J.; Ramalho, T.; Grabska-Barwinska, A.; et al. 2017. Overcoming catastrophic forgetting in neural networks. *Proceedings of the national academy of sciences*, 114(13): 3521–3526.

Liu, H.; Yang, Y.; and Wang, X. 2021. Overcoming catastrophic forgetting in graph neural networks. In *Proceedings of the AAAI Conference on Artificial Intelligence*, volume 35, 8653–8661.

Lopez-Paz, D.; and Ranzato, M. 2017. Gradient episodic memory for continual learning. *Advances in neural information processing systems*, 30.

Marcos Alvarez, A.; Wehenkel, L.; and Louveaux, Q. 2016. Online learning for strong branching approximation in branch-and-bound.

Nair, V.; Bartunov, S.; Gimeno, F.; von Glehn, I.; Lichocki, P.; Lobov, I.; O'Donoghue, B.; Sonnerat, N.; Tjandraatmadja, C.; Wang, P.; et al. 2020. Solving mixed integer programs using neural networks. *arXiv preprint arXiv:2012.13349*.

Parisi, G. I.; Kemker, R.; Part, J. L.; Kanan, C.; and Wermter, S. 2019. Continual lifelong learning with neural networks: A review. *Neural Networks*, 113: 54–71.

Rebuffi, S.-A.; Kolesnikov, A.; Sperl, G.; and Lampert, C. H. 2017. icarl: Incremental classifier and representation learning. In *Proceedings of the IEEE conference on Computer Vision and Pattern Recognition*, 2001–2010.

Riemer, M.; Cases, I.; Ajemian, R.; Liu, M.; Rish, I.; Tu, Y.; and Tesauro, G. 2018. Learning to learn without forgetting by maximizing transfer and minimizing interference. *arXiv preprint arXiv:1810.11910*.

Taha, H. A. 2014. *Integer programming: theory, applications, and computations*.

Vaswani, A.; Shazeer, N.; Parmar, N.; Uszkoreit, J.; Jones, L.; Gomez, A. N.; Kaiser, Ł.; and Polosukhin, I. 2017. Attention is all you need. *Advances in neural information processing systems*, 30.

Wang, J.; Song, G.; Wu, Y.; and Wang, L. 2020. Streaming graph neural networks via continual learning. In *Proceedings of the 29th ACM International Conference on Information & Knowledge Management*, 1515–1524.

Yoon, J.; Yang, E.; Lee, J.; and Hwang, S. J. 2017. Lifelong learning with dynamically expandable networks. *arXiv preprint arXiv:1708.01547*.

Zarpellon, G.; Jo, J.; Lodi, A.; and Bengio, Y. 2020. Parameterizing branch-and-bound search trees to learn branching policies. *arXiv preprint arXiv:2002.05120*.

Zenke, F.; Poole, B.; and Ganguli, S. 2017. Continual learning through synaptic intelligence. In *International Conference on Machine Learning*, 3987–3995. PMLR.

Zhou, F.; and Cao, C. 2021. Overcoming catastrophic forgetting in graph neural networks with experience replay. In *Proceedings of the AAAI Conference on Artificial Intelligence*, volume 35, 4714–4722.

A Appendix

A.1 Related Work

A.2 Learning to solve MIPs

Strong Branching is widely accepted as the most efficient branching expert in terms of number of nodes. However, its main advantage is the high computational cost of finding the variable to branch. To tackle this problem, Learning-based techniques(Alvarez, Louveaux, and Wehenkel 2014, 2017; Marcos Alvarez, Wehenkel, and Louveaux 2016; Khalil et al. 2016; Gasse et al. 2019; Nair et al. 2020; Gupta et al. 2020) have focused on learning fast approximations of *Strong Branching* rule by learning from a set of training instances for a class of MIPs. Most of these techniques either learn to rank candidate branching variables or learn to imitate expert strong branching rule. Among various learning based methods, GCNN(Gasse et al. 2019) has shown significant scalability gains and is considered the state-of-the-art method for learning to branching(Banitalebi-Dehkordi and Zhang 2021). It has shown to improve upon previously proposed approaches for branching on several MILP problem benchmarks, and further, also obtains faster running time compared to the default SCIP solver. Recently, (Zarpellon et al. 2020) proposed *TreeGate* model to learn approximation of reliability pseudo-cost branching. However, in our study we observed, the technique does not scale well in comparison to GCNN(Gasse et al. 2019) and default SCIP solver in terms of the running time metric. Recently, there have been attempts to use reinforcement learning to obtain better heuristics⁴, however, in terms of running time they are still inferior to imitation learning of strong branching.

A.3 Continual Learning

Although deep neural networks have obtained significant success on sever learning tasks, however most of them suffer from catastrophic forgetting in the continual learning scenario. The goal of continual learning is to learn to adapt to new data in a streaming scenario while consolidating the knowledge learned from previous data to prevent catastrophic forgetting. Many recent endeavours have been made towards alleviating catastrophic forgetting. The first one’s being replay-based(Rebuffi et al. 2017; Riemer et al. 2018; Lopez-Paz and Ranzato 2017; Chaudhry et al. 2018) where a subset of old data samples are replayed from a memory buffer while learning a new task. Second category is the regularization based techniques(Zenke, Poole, and Ganguli 2017; Kirkpatrick et al. 2017; Aljundi et al. 2018) which learn importance of weights of the neural model for each task and prevent significant changes on them. The third category is dynamic network expansion. In this context, some progress has been made to intelligently expand the neural network(Yoon et al. 2017; Draeos et al. 2017) when the current capacity of the model is not sufficient to learn new tasks without causing forgetting of earlier one’s. These approaches introduced here change architectural properties in

⁴Scavuzzo, L. Learning to branch with Tree MDPs. arXiv preprint arXiv:2205.11107.

response to new information by dynamically accommodating novel neural resources with due course of time such as increased number of neurons or network layers. Recently, some amount of progress has been made on continual learning on GNNs(Wang et al. 2020; Liu, Yang, and Wang 2021; Zhou and Cao 2021). We refer the reader to the follow surveys on continual learning on neural networks(Parisi et al. 2019) and continual learning for GNNs(Febrinanto et al. 2022).

A.4 Solver Features

In Table 3 we present the input features used. These features are based upon Gasse et al. (2019).

A.5 Multi-head attention

The multi-head attention equation is based upon Vaswani et al. (2017). Specifically, for K heads

$$\vec{h}'_i = \parallel_{k=1}^K \rho \left(\sum_{j \in \mathcal{N}(i)} \alpha_{ij}^k \mathbf{W}^k \vec{h}_j \right)$$

where h_i can be replaced by c_i or v_i and \mathbf{W} be replaced with θ^C or θ^V respectively.

A.6 Data

Facility location: For facility location, as discussed the main paper, a certain task of facility location problem is defined as $FC_{(Clow,Chigh),(Dlow,Dhigh)}$. *Clow*, *Chigh* refers to the lower and upper limit(respectively) of the facility capacity. *Dlow*, *Dhigh* refers to the lower and upper limit(respectively) of the customer demand . To generate an instance of the facility location problem, we require, for each facility, sampling a capacity uniformly at random from $[Clow, Chigh]$ and for each customer a demand sampled uniformly at random from $[Dlow, Dhigh]$. Using these values, an instance is constructed. In addition to evolving customer demand and facility supply distribution, we also simulate the setting of adding new constraints. We add the constraint of the maximum number of customers that can be served by a facility and denote it by MS . For example $MS = 95$ in $FC_{(100,110),(80,90),MS=95}$ denotes that maximum number of customers that can be served by a facility is 95. In all cases, we set the number of customers and facilities for an instance to be 100.

A.7 Parameters

We set number of heads to 2 for multi-head attention with MLP hidden size 32. We train until convergence of validation loss. We set learning rate to 0.001. We use Adam optimizer for training.

A.8 Baselines

For EWC baseline(only using EWC), we set weight of the *elastic weight* component to 1000. For GCNN we use embedding size 64.

Tensor	Feature	Description
C	obj_cos_sim	Cosine similarity with objective.
	bias	Bias value, normalized with constraint coefficients.
	dualsol_val	Dual solution value, normalized.
	is_tight	Tightness indicator in LP solution
	age	LP age, normalized with total number of LPs
E	Coef	Constraint coefficient, normalized per constraint
V	type	Type (binary, integer, impl. integer, continuous) as a one-hot encoding
	coef	Objective coefficient, normalized
	has_lb	Lower bound indicator.
	has_ub	Upper bound indicator.
	sol_is_at_lb	Solution value equals lower bound.
	sol_is_at_ub	Solution value equals upper bound
	sol_frac	Solution value fractionality
	basis_status	Simplex basis status (lower, basic, upper, zero) as a one-hot encoding
	reduced_cost	Reduced cost, normalized
	age	LP age, normalized
	sol_val	Solution value.
	inc_val	Value in incumbent
	avg_inc_val	Average value in incumbents

Table 3: Description of the constraint, edge and variable features in our bipartite state representation s_t

A.9 Number of nodes

In addition to plots based upon solving time shown in the main paper, in fig. 6 and 7, we present the number of nodes solved for different methods.

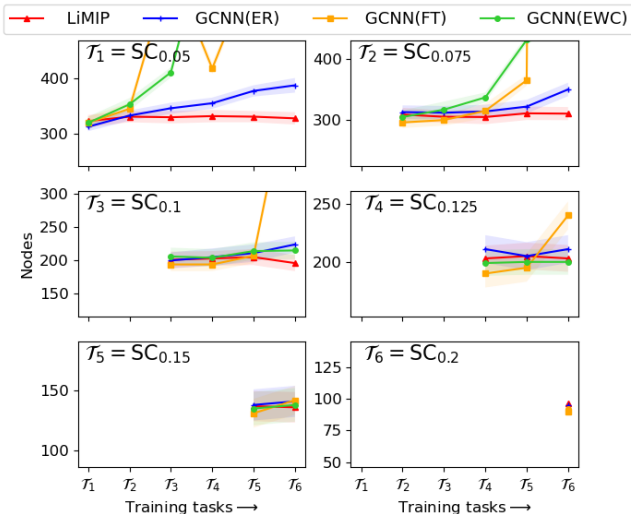


Figure 6: **Number of Nodes: Testing on SetCover in lifelong scenario:** Evolution of number of nodes for each task when different methods are updated on each task sequentially.

A.10 Additional Results

Results on Independent Set We present the results on Independent set problem in fig 8. We observe that in independent set also, LiMIP achieves significant lower forgetting in

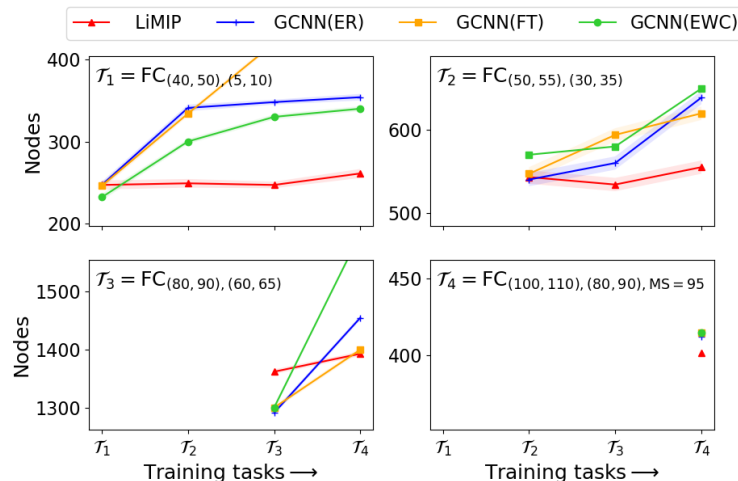


Figure 7: **Number of Nodes: Testing on Facility location in lifelong scenario:** Evolution of number of nodes for each task when different methods are updated on each task sequentially.

comparison to other methods. Standard deviation on Independent set is significantly high, a phenomenon observed in earlier works too (Gasse et al. 2019).

Results on default SCIP solver heuristics : For the sake of completeness we present results of SCIP solver in table 4. We skip results of fsb for $FC_{(40,50),(5,10)}$ due to its poor running time performance.

A.11 Poor scalability of TreeGate (Zarpellon et al. 2020)

We test the performance of TreeGate (Zarpellon et al. 2020) in our setup where we have a set of training instances avail-

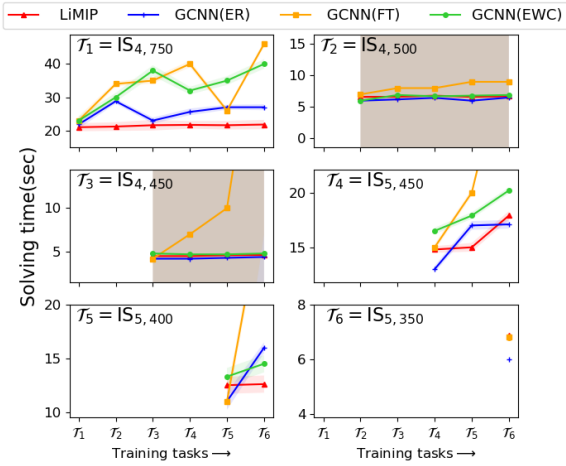


Figure 8: **Independent Set: Testing on Independent Set in lifelong scenario:** Evolution of solving time for each task when different methods are updated on each task sequentially.

Dataset	Method	Time	Nodes
$SC_{0.05}$	relpscost	9.93 ± 1.1	497.2 ± 16.1
	fsb	63.50 ± 2.1	91.5 ± 4.5
$IS_{4,750}$	relpscost	66.2 ± 0.1	21010 ± 1.2
	fsb	1531.50 ± 0.15	1195.5 ± 0.1
$FC_{(40,50),(5,10)}$	relpscost	268.2 ± 0.88	7528 ± 0.62

Table 4: Results of SCIP Full Strong (fsb) and SCIP Reliability pseudocost(relpscost) branching

able for a class of MIP. We generate relpscost branching pairs from the $SC_{0.05}$ dataset similar to procedure described in (Zarpellon et al. 2020) i.e using different random seeds and also performing random branching. We used same set of training instances as used in LiMIP and GCNN to generate branching pairs.

We compare the running time and number of nodes. In Table 5 we observe that TreeGate is twice slower compared to imitation learning of strong branching.

Model	Time	# Nodes
TreeGate	24.1	764
LiMIP (Bipartite GAT)	11.01	320

Table 5: **Comparison against TreeGate(Zarpellon et al. 2020):** Comparison of Imitation learning of Strong Branching against TreeGate which learns weaker heuristic of reliability pseudo cost branching. Both models were trained and tested on $SC_{0.05}$.

A.12 Ablation

LiMIP without Elastic weight consolidation In fig. 9 we study the performance of LiMIP without the EWC loss. We observe that there does exist improvement when EWC loss is part of our loss function $\mathcal{L}_{lifelong}$.

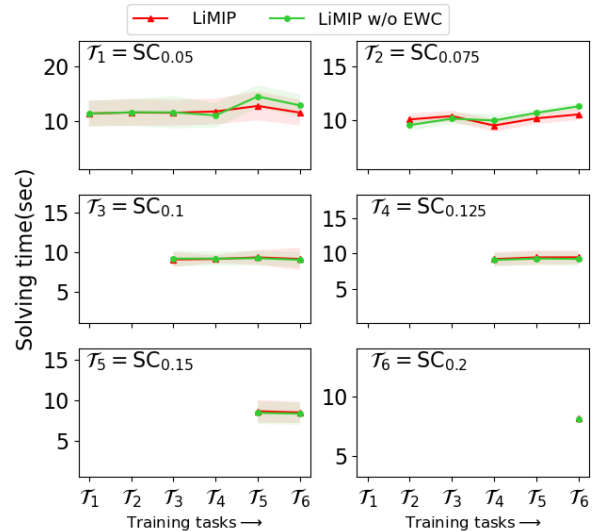


Figure 9: **LiMIP without EWC: Testing on SetCover in lifelong scenario:** Evolution of Solving time for each task when different methods are updated on each task sequentially.

Using small sized memory buffer: We use a buffer of size 200 instead of 500 used earlier. We observe similar conclusion on a lower buffer size as can be seen in fig. 10. For simplicity, we show result on the first and the last problem in the facility location problem sequence.

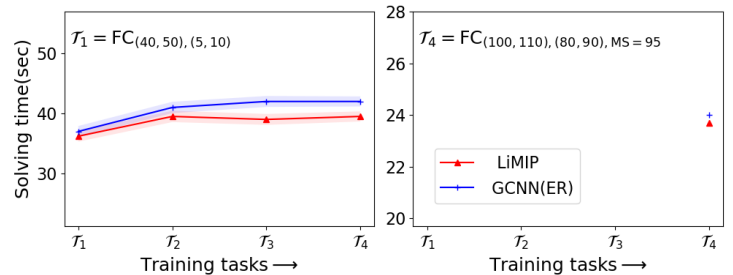


Figure 10: **Comparison of LiMIP and ER model on buffer size 200:** Testing on first and last problem in the Facility location problem sequence.

Using Bipartite GAT encoding for baselines instead of GCNN In fig. 11 and 12 we study the performance of different baselines when the base model used for them is bipartite GAT. This shows that LiMIP outperforms existing baselines irrespective of the GNN encoding used. We

observe similar conclusion as observed on GCNN in main paper.

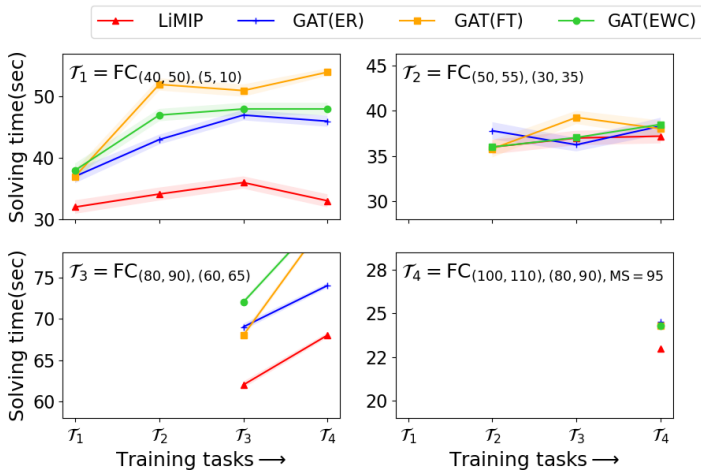


Figure 11: **Comparison using Bipartite GAT as encoding model for baselines: Testing on Facility location in lifelong scenario:** Evolution of solving time for each task when different methods are updated on each task sequentially.

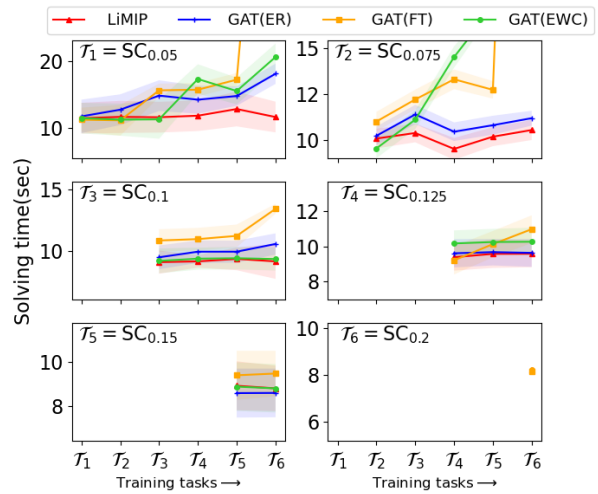


Figure 12: **Comparison using encoding model as Bipartite GAT for baselines : Testing on SetCover in lifelong scenario:** Evolution of solving time for each task when different methods are updated on each task sequentially.